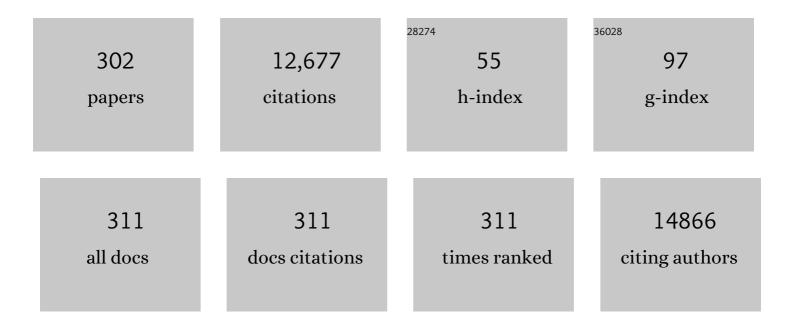
List of Publications by Year in descending order

Source: https://exaly.com/author-pdf/3178466/publications.pdf Version: 2024-02-01



#	Article	IF	CITATIONS
1	Virus-Enabled Synthesis and Assembly of Nanowires for Lithium Ion Battery Electrodes. Science, 2006, 312, 885-888.	12.6	1,756
2	Gas sensing properties of defect-controlled ZnO-nanowire gas sensor. Applied Physics Letters, 2008, 93, .	3.3	643
3	Investigation of the relations between structure and microwave dielectric properties of divalent metal tungstate compounds. Journal of the European Ceramic Society, 2006, 26, 2051-2054.	5.7	314
4	Highly Conductive Coaxial SnO <sub>2</sub> â^'ln <sub>2</sub> O <sub>3</sub> Heterostructured Nanowires for Li Ion Battery Electrodes. Nano Letters, 2007, 7, 3041-3045.	9.1	312
5	On-chip fabrication of ZnO-nanowire gas sensor with high gas sensitivity. Sensors and Actuators B: Chemical, 2009, 138, 168-173.	7.8	303
6	Highly Reversible Lithium Storage in Bacillus subtilis-Directed Porous Co <sub>3</sub> O <sub>4</sub> Nanostructures. ACS Nano, 2011, 5, 443-449.	14.6	185
7	Synthesis of Cu <sub>2</sub> PO <sub>4</sub> OH Hierarchical Superstructures with Photocatalytic Activity in Visible Light. Advanced Functional Materials, 2008, 18, 2154-2162.	14.9	141
8	Electrocatalytic Selective Oxygen Evolution of Carbon-Coated Na <sub>2</sub> Co <sub>1–<i>x</i></sub> Fe <sub><i>x</i></sub> P <sub>2</sub> O <sub>7</sub> Nanoparticles for Alkaline Seawater Electrolysis. ACS Catalysis, 2020, 10, 702-709.	11.2	141
9	Self-supported SnO <sub>2</sub> nanowire electrodes for high-power lithium-ion batteries. Nanotechnology, 2009, 20, 455701.	2.6	129
10	Dielectric properties of Ln(Mg <sub>1/2</sub> Ti <sub>1/2</sub> )O <sub>3</sub> as substrates for high-T <sub><i>c</i></sub> superconductor thin films. Journal of Materials Research, 1999, 14, 2484-2487.	2.6	120
11	Repeated-oral dose toxicity of polyethylene microplastics and the possible implications on reproduction and development of the next generation. Toxicology Letters, 2020, 324, 75-85.	0.8	120
12	Microwave Dielectric Properties of Rare-Earth Ortho-Niobates with Ferroelasticity. Journal of the American Ceramic Society, 2006, 89, 3861-3864.	3.8	118
13	Phase Relations and Microwave Dielectric Properties of ZnNb <sub>2</sub> O <sub>6</sub> –TiO <sub>2</sub> . Journal of Materials Research, 2000, 15, 1331-1335.	2.6	117
14	Scalable One-pot Bacteria-templating Synthesis Route toward Hierarchical, Porous-Co3O4 Superstructures for Supercapacitor Electrodes. Scientific Reports, 2013, 3, 2325.	3.3	109
15	"Brain oral‣ike―Mesoporous Hollow CoS <sub>2</sub> @Nâ€Doped Graphitic Carbon Nanoshells as Efficient Sulfur Reservoirs for Lithium–Sulfur Batteries. Advanced Functional Materials, 2019, 29, 1903712.	14.9	108
16	3D Architectures of Quaternary Coâ€Niâ€&â€P/Graphene Hybrids as Highly Active and Stable Bifunctional Electrocatalysts for Overall Water Splitting. Advanced Energy Materials, 2018, 8, 1802319.	19.5	107
17	Influence of Copper(II) Oxide Additions to Zinc Niobate Microwave Ceramics on Sintering Temperature and Dielectric Properties. Journal of the American Ceramic Society, 2001, 84, 1286-1290.	3.8	105
18	Microwave Dielectric Properties of Lowâ€Fired ZnNb <sub>2</sub> O <sub>6</sub> Ceramics with BiVO <sub>4</sub> Addition. Journal of the American Ceramic Society, 2004, 87, 871-874.	3.8	98

#	Article	IF	CITATIONS
19	Low-temperature firing and microwave dielectric properties of BaTi4O9 with Zn-B-O glass system. Materials Research Bulletin, 2001, 36, 585-595.	5.2	97
20	Glass-free LTCC microwave dielectric ceramics. Materials Research Bulletin, 2005, 40, 2120-2129.	5.2	97
21	RbBaPO <sub>4</sub> :Eu <sup>2+</sup> : a new alternative blue-emitting phosphor for UV-based white light-emitting diodes. Journal of Materials Chemistry C, 2013, 1, 500-505.	5.5	96
22	Superior rate capabilities of SnS nanosheet electrodes for Li ion batteries. Electrochemistry Communications, 2010, 12, 307-310.	4.7	92
23	Highly Efficient Perovskiteâ€Based Electrocatalysts for Water Oxidation in Acidic Environments: A Mini Review. Advanced Energy Materials, 2021, 11, 2002428.	19.5	92
24	A binder-free Ge-nanoparticle anode assembled on multiwalled carbon nanotube networks for Li-ion batteries. Chemical Communications, 2012, 48, 7061.	4.1	90
25	Toxic response of graphene nanoplatelets in vivo and in vitro. Archives of Toxicology, 2015, 89, 1557-1568.	4.2	86
26	Mixture behavior and microwave dielectric properties of (1â^'x)CaWO4–xTiO2. Journal of the European Ceramic Society, 2007, 27, 3087-3091.	5.7	84
27	Novel one-pot route to monodisperse thermosensitive hollow microcapsules in a microfluidic system. Lab on A Chip, 2008, 8, 1544.	6.0	80
28	Microwave Dielectric Properties of A2P2O7(A = Ca, Sr, Ba; Mg, Zn, Mn). Japanese Journal of Applied Physics, 2004, 43, 3521-3525.	1.5	79
29	Low-temperature sintering and microwave dielectric properties of Ba5Nb4O15–BaNb2O6 mixtures for LTCC applications. Journal of the European Ceramic Society, 2003, 23, 2597-2601.	5.7	78
30	Long-term, high-rate lithium storage capabilities of TiO2 nanostructured electrodes using 3D self-supported indium tin oxide conducting nanowire arrays. Energy and Environmental Science, 2011, 4, 1796.	30.8	76
31	Enhanced Li Storage Capacity in 3 nm Diameter SnO <sub>2</sub> Nanocrystals Firmly Anchored on Multiwalled Carbon Nanotubes. Journal of Physical Chemistry C, 2011, 115, 22062-22067.	3.1	76
32	Microwave dielectric properties of Ca2P2O7. Journal of the European Ceramic Society, 2003, 23, 2589-2592.	5.7	75
33	Formation of Lithiumâ€Driven Active/Inactive Nanocomposite Electrodes Based on Ca <sub>3</sub> Co <sub>4</sub> O <sub>9</sub> Nanoplates. Angewandte Chemie - International Edition, 2007, 46, 6654-6657.	13.8	75
34	Observation of ferroelectromagnetic nature in rare-earth-substituted bismuth iron titanate. Applied Physics Letters, 2003, 83, 2217-2219.	3.3	74
35	Wolframite-type ZnWO <sub>4</sub> Nanorods as New Anodes for Li-Ion Batteries. Journal of Physical Chemistry C, 2011, 115, 16228-16233.	3.1	74
36	Mixture Behavior and Microwave Dielectric Properties in the Low-fired TiO2–CuO System. Japanese Journal of Applied Physics, 2000, 39, 2696-2700.	1.5	73

#	Article	IF	CITATIONS
37	Phase Constitutions and Microwave Dielectric Properties of Zn3Nb2O8–TiO2. Japanese Journal of Applied Physics, 2001, 40, 5994-5998.	1.5	73
38	Study of magnetic and magnetoelectric measurements in bismuth iron titanate ceramic—Bi8Fe4Ti3O24. Materials Research Bulletin, 2004, 39, 55-61.	5.2	72
39	Preparation of Brookiteâ€Type TiO <sub>2</sub> /Carbon Nanocomposite Electrodes for Application to Li Ion Batteries. European Journal of Inorganic Chemistry, 2008, 2008, 878-882.	2.0	72
40	Highly Reversible Li Storage in Hybrid NiO/Ni/Graphene Nanocomposites Prepared by an Electrical Wire Explosion Process. ACS Applied Materials & Interfaces, 2014, 6, 137-142.	8.0	69
41	Facile hydrothermal synthesis of porous TiO <sub>2</sub> nanowire electrodes with high-rate capability for Li ion batteries. Nanotechnology, 2010, 21, 255706.	2.6	68
42	Sn-induced low-temperature growth of Ge nanowire electrodes with a large lithium storage capacity. Nanoscale, 2011, 3, 3371.	5.6	67
43	Fast adsorption kinetics of highly dispersed ultrafine nickel/carbon nanoparticles for organic dye removal. Applied Surface Science, 2018, 439, 364-370.	6.1	67
44	Voltage tunable dielectric properties of rf sputtered Bi2O3-ZnO-Nb2O5 pyrochlore thin films. Thin Solid Films, 2002, 419, 183-188.	1.8	65
45	An approach to flexible Na-ion batteries with exceptional rate capability and long lifespan using Na <sub>2</sub> FeP <sub>2</sub> O <sub>7</sub> nanoparticles on porous carbon cloth. Journal of Materials Chemistry A, 2017, 5, 5502-5510.	10.3	64
46	Low-temperature sintering and microwave dielectric properties of BaO·(Nd1â^'xBix)2O3·4TiO2 by the glass additions. Ceramics International, 2004, 30, 1181-1185.	4.8	61
47	Synthesis of core/shell spinel ferrite/carbon nanoparticles with enhanced cycling stability for lithium ion battery anodes. Nanotechnology, 2012, 23, 125402.	2.6	61
48	Low-firing of CuO-doped anatase. Materials Research Bulletin, 1999, 34, 771-781.	5.2	60
49	Enhancement of cyclability of urchin-like rutile TiO2 submicron spheres by nanopainting with carbon. Journal of Materials Chemistry, 2012, 22, 15981.	6.7	60
50	Heteroepitaxial growth of ZnO nanosheet bands on ZnCo2O4 submicron rods toward high-performance Li ion battery electrodes. Nano Research, 2013, 6, 348-355.	10.4	60
51	Peroxymonosulfate activation by carbon-encapsulated metal nanoparticles: Switching the primary reaction route and increasing chemical stability. Applied Catalysis B: Environmental, 2020, 279, 119360.	20.2	60
52	Origin of Capacity Fading in Nano-Sized Co3O4Electrodes: Electrochemical Impedance Spectroscopy Study. Nanoscale Research Letters, 2008, 3, .	5.7	58
53	Enhanced cycling performance of an Fe0/Fe3O4nanocomposite electrode for lithium-ion batteries. Nanotechnology, 2009, 20, 295205.	2.6	58
54	Luminescence properties of Ca5(PO4)2SiO4:Eu2+ green phosphor for near UV-based white LED. Materials Letters, 2012, 70, 37-39.	2.6	58

#	Article	IF	CITATIONS
55	Microwave Dielectric Properties of Lowâ€Fired Ba <sub>5</sub> Nb <sub>4</sub> O <sub>15</sub> . Journal of the American Ceramic Society, 2002, 85, 2759-2762.	3.8	57
56	Synthesis of multiphase SnSb nanoparticles-on-SnO2/Sn/C nanofibers for use in Li and Na ion battery electrodes. Electrochemistry Communications, 2014, 46, 124-127.	4.7	56
57	Porous Lithiophilic Li–Si Alloyâ€Type Interfacial Framework via Selfâ€Discharge Mechanism for Stable Lithium Metal Anode with Superior Rate. Advanced Energy Materials, 2021, 11, 2101544.	19.5	56
58	Origin of Microwave Dielectric Loss in ZnNb <sub>2</sub> O <sub>6</sub> â€TiO <sub>2</sub> . Journal of the American Ceramic Society, 2002, 85, 1169-1172.	3.8	55
59	Interaction of BiNbO <sub>4</sub> â€Based Lowâ€Firing Ceramics with Silver Electrodes. Journal of the American Ceramic Society, 1998, 81, 3038-3040.	3.8	54
60	Effects of carbon content on the photocatalytic activity of C/BiVO4 composites under visible light irradiation. Materials Chemistry and Physics, 2010, 119, 106-111.	4.0	54
61	Carbon-encapsulated NiFe nanoparticles as a bifunctional electrocatalyst for high-efficiency overall water splitting. Journal of Catalysis, 2018, 366, 266-274.	6.2	54
62	Ultrafine αâ€Phase Molybdenum Carbide Decorated with Platinum Nanoparticles for Efficient Hydrogen Production in Acidic and Alkaline Media. Advanced Science, 2019, 6, 1802135.	11.2	54
63	Cobalt phosphide nanoarrays with crystalline-amorphous hybrid phase for hydrogen production in universal-pH. Nano Research, 2020, 13, 2469-2477.	10.4	54
64	MnMoO <sub>4</sub> Electrocatalysts for Superior Long‣ife and Highâ€Rate Lithiumâ€Oxygen Batteries. Advanced Energy Materials, 2017, 7, 1601741.	19.5	53
65	CeO2/Co(OH)2 hybrid electrocatalysts for efficient hydrogen and oxygen evolution reaction. Journal of Alloys and Compounds, 2019, 800, 450-455.	5.5	53
66	Phase transformation and microwave dielectric properties of BiPO4 ceramics. Journal of Electroceramics, 2006, 16, 379-383.	2.0	51
67	A graphite foil electrode covered with electrochemically exfoliated graphene nanosheets. Electrochemistry Communications, 2010, 12, 1419-1422.	4.7	51
68	Synthesis of pseudobrookite-type Fe2TiO5 nanoparticles and their Li-ion electroactivity. Ceramics International, 2012, 38, 6009-6013.	4.8	51
69	Stable field emission performance of SiC-nanowire-based cathodes. Nanotechnology, 2008, 19, 225706.	2.6	50
70	Magnéli-Phase Ti <sub>4</sub> O <sub>7</sub> Nanosphere Electrocatalyst Support for Carbon-Free Oxygen Electrodes in Lithium–Oxygen Batteries. ACS Catalysis, 2018, 8, 2601-2610.	11.2	50
71	Onion-like crystalline WS2 nanoparticles anchored on graphene sheets as high-performance anode materials for lithium-ion batteries. Chemical Engineering Journal, 2019, 375, 122033.	12.7	49
72	High-power and long-life supercapacitive performance of hierarchical, 3-D urchin-like W18O49 nanostructure electrodes. Nano Research, 2016, 9, 633-643.	10.4	47

#	Article	IF	CITATIONS
73	Microwave dielectric properties of (1 â^' x)Cu3Nb2O8â^'xZn3Nb2O8 ceramics. Journal of Materials Research, 2001, 16, 1465-1470.	2.6	46
74	Low-temperature sintering of temperature-stable LaNbO4 microwave dielectric ceramics. Materials Research Bulletin, 2010, 45, 21-24.	5.2	46
75	Low-temperature synthesis of CuO-interlaced nanodiscs for lithium ion battery electrodes. Nanoscale Research Letters, 2011, 6, 397.	5.7	46
76	Electrochemical performance of Ni x Co1-xMoO4 (0 ≤ ≤) nanowire anodes for lithium-ion batteries. Nanoscale Research Letters, 2012, 7, 35.	5.7	46
77	Visible-Light-Induced Photocatalytic Activity in FeNbO <sub>4</sub> Nanoparticles. Journal of Physical Chemistry C, 2008, 112, 18393-18398.	3.1	45
78	Sb:SnO <sub>2</sub> @TiO <sub>2</sub> Heteroepitaxial Branched Nanoarchitectures for Li Ion Battery Electrodes. Journal of Physical Chemistry C, 2012, 116, 21717-21726.	3.1	45
79	Three-dimensional hierarchical self-supported multi-walled carbon nanotubes/tin(iv) disulfide nanosheets heterostructure electrodes for high power Li ion batteries. Journal of Materials Chemistry, 2012, 22, 9330.	6.7	44
80	Direct assembly of tin–MWCNT 3D-networked anode for rechargeable lithium ion batteries. RSC Advances, 2012, 2, 3315.	3.6	44
81	1D/2D carbon nanotube/graphene nanosheet composite anodes fabricated using electrophoretic assembly. Ceramics International, 2012, 38, 3017-3021.	4.8	43
82	Biodistribution and toxicity of spherical aluminum oxide nanoparticles. Journal of Applied Toxicology, 2016, 36, 424-433.	2.8	42
83	Amorphous hydrated vanadium oxide with enlarged interlayer spacing for aqueous zinc-ion batteries. Chemical Engineering Journal, 2021, 420, 130528.	12.7	42
84	Room-temperature synthesis of CuO/graphene nanocomposite electrodes for high lithium storage capacity. Ceramics International, 2013, 39, 1749-1755.	4.8	41
85	Microwave dielectric properties of (Ca1â^'xZnx)2P2O7. Materials Letters, 2005, 59, 257-260.	2.6	40
86	Low-temperature sintering and microwave dielectric properties of Ba5Nb4O15 with ZnB2O4 glass. Journal of the European Ceramic Society, 2006, 26, 2105-2109.	5.7	40
87	Enhanced photoluminescence property of Dy3+ co-doped BaAl2O4:Eu2+ green phosphors. Ceramics International, 2012, 38, 443-447.	4.8	40
88	Tailoring uniform Î <sup>3</sup> -MnO2 nanosheets on highly conductive three-dimensional current collectors for high-performance supercapacitor electrodes. Nano Research, 2015, 8, 990-1004.	10.4	39
89	High-areal-capacity lithium storage of the Kirkendall effect-driven hollow hierarchical NiSxnanoarchitecture. Nanoscale, 2015, 7, 2790-2796.	5.6	38
90	Waste Windshield-Derived Silicon/Carbon Nanocomposites as High-Performance Lithium-Ion Battery Anodes. Scientific Reports, 2018, 8, 960.	3.3	38

#	Article	IF	CITATIONS
91	Influence of Anatase–Rutile Phase Transformation on Dielectric Properties of Sol–Gel Derived TiO2Thin Films. Japanese Journal of Applied Physics, 2005, 44, 6148-6151.	1.5	37
92	Tailoring high-surface-area nanocrystalline TiO2 polymorphs for high-power Li ion battery electrodes. Electrochimica Acta, 2010, 55, 7315-7321.	5.2	37
93	Biomineralized Sn-based multiphasic nanostructures for Li-ion battery electrodes. Nanoscale, 2012, 4, 4694.	5.6	37
94	Hierarchical assembly of TiO2–SrTiO3 heterostructures on conductive SnO2 backbone nanobelts for enhanced photoelectrochemical and photocatalytic performance. Journal of Hazardous Materials, 2014, 275, 10-18.	12.4	37
95	Highly stable sodium storage in 3-D gradational Sb–NiSb–Ni heterostructures. Nano Energy, 2015, 15, 479-489.	16.0	37
96	Enhanced Lithium Storage in Hierarchically Porous Carbon Derived from Waste Tea Leaves. Scientific Reports, 2016, 6, 39099.	3.3	37
97	Synergistic Effect of CuGeO <sub>3</sub> /Graphene Composites for Efficient Oxygen–Electrode Electrocatalysts in Li–O <sub>2</sub> Batteries. Advanced Energy Materials, 2018, 8, 1801930.	19.5	37
98	Synthesis of Heterogeneous Li4Ti5O12 Nanostructured Anodes with Long-Term Cycle Stability. Nanoscale Research Letters, 2010, 5, 1585-1589.	5.7	36
99	Phase analysis and microwave dielectric properties of LTCC TiO2 with glass system. Journal of the European Ceramic Society, 2003, 23, 2549-2552.	5.7	35
100	Size-controlled synthesis of monodispersed mesoporous α-Alumina spheres by a template-free forced hydrolysis method. Dalton Transactions, 2011, 40, 6901.	3.3	35
101	Mo-MoO3-graphene nanocomposites as anode materials for lithium-ion batteries: scalable, facile preparation and characterization. Electrochimica Acta, 2017, 251, 81-90.	5.2	35
102	In Situ Conversion of Metal–Organic Frameworks into VO <sub>2</sub> –V <sub>3</sub> S <sub>4</sub> Heterocatalyst Embedded Layered Porous Carbon as an "Allâ€inâ€One―Host for Lithium–Sulfur Batteries. Small, 2020, 16, e2004806.	10.0	35
103	Metal-organic-framework-derived 3D crumpled carbon nanosheets with self-assembled CoxSy nanocatalysts as an interlayer for lithium-sulfur batteries. Chemical Engineering Journal, 2020, 400, 125959.	12.7	35
104	Sn self-doped α-Fe2O3 nanobranch arrays supported on a transparent, conductive SnO2 trunk to improve photoelectrochemical water oxidation. International Journal of Hydrogen Energy, 2014, 39, 16459-16467.	7.1	34
105	Structural and electrochemical characteristics of morphology-controlled Li[Ni0.5Mn1.5]O4 cathodes. Electrochimica Acta, 2015, 156, 29-37.	5.2	34
106	Tailored silicon hollow spheres with Micrococcus for Li ion battery electrodes. Chemical Engineering Journal, 2017, 327, 297-306.	12.7	34
107	Structural Transition and Microwave Dielectric Properties of ZnNb2O6–TiO2Sintered at Low Temperatures. Japanese Journal of Applied Physics, 2002, 41, 1465-1469.	1.5	33
108	Comparison of toxicity between the different-type TiO2 nanowires in vivo and in vitro. Archives of Toxicology, 2013, 87, 1219-1230.	4.2	33

#	Article	IF	CITATIONS
109	Superior long-life and high-rate Ge nanoarrays anchored on Cu/C nanowire frameworks for Li-ion battery electrodes. Nano Energy, 2015, 13, 218-225.	16.0	33
110	Enhanced Rate Capabilities of Nanobrookite with Electronically Conducting MWCNT Networks. Crystal Growth and Design, 2008, 8, 4506-4510.	3.0	32
111	3D Architectures of Co <i><sub>x</sub></i> P Using Silk Fibroin Scaffolds: An Active and Stable Electrocatalyst for Hydrogen Generation in Acidic and Alkaline Media. Small, 2018, 14, e1801284.	10.0	32
112	Phase transformation and sintering behavior of Ca2P2O7. Materials Letters, 2004, 58, 347-351.	2.6	31
113	Microwave dielectric properties and low-temperature sintering of Ba3Ti4Nb4O21 ceramics with B2O3 and CuO additions. Journal of the European Ceramic Society, 2007, 27, 3053-3057.	5.7	31
114	Superior anodic oxidation in tailored Sb-doped SnO2/RuO2 composite nanofibers for electrochemical water treatment. Journal of Catalysis, 2019, 374, 118-126.	6.2	31
115	Li electroactivity of iron (II) tungstate nanorods. Nanotechnology, 2010, 21, 465602.	2.6	30
116	Kinetic insight into perovskite <scp>La<sub>0.8</sub>Sr<sub>0.2</sub>VO<sub>3</sub></scp> nanofibers as an efficient electrocatalytic cathode for highâ€rate <scp>LiO<sub>2</sub></scp> batteries. InformaÄnÃ-Materiály, 2021, 3, 1295-1310.	17.3	30
117	SrNb2O6 nanotubes with enhanced photocatalytic activity. Journal of Materials Chemistry, 2010, 20, 3979.	6.7	28
118	Superior lithium storage in nitrogen-doped carbon nanofibers with open-channels. Chemical Engineering Journal, 2017, 315, 1-9.	12.7	28
119	Pulmonary persistence of graphene nanoplatelets may disturb physiological and immunological homeostasis. Journal of Applied Toxicology, 2017, 37, 296-309.	2.8	28
120	Waste glass microfiber filter-derived fabrication of fibrous yolk-shell structured silicon/carbon composite freestanding electrodes for lithium-ion battery anodes. Journal of Power Sources, 2020, 468, 228407.	7.8	28
121	Uniform Si nanoparticle-embedded nitrogen-doped carbon nanofiber electrodes for lithium ion batteries. Journal of Alloys and Compounds, 2017, 728, 490-496.	5.5	27
122	Mechanically Interlocked Polymer Electrolyte with Builtâ€in Fast Molecular Shuttles for Allâ€Solidâ€State Lithium Batteries. Advanced Energy Materials, 2021, 11, 2102583.	19.5	27
123	Microwave Dielectric Properties of (1-x)Ba5Nb4O15–xBaNb2O6Mixtures. Japanese Journal of Applied Physics, 2002, 41, 3812-3816.	1.5	26
124	Low temperature sintering and microwave dielectric properties of Ba3Ti5Nb6O28 with ZnO–B2O3 glass additions for LTCC applications. Journal of the European Ceramic Society, 2007, 27, 3075-3079.	5.7	26
125	Synthesis of manganese oxide nanostructures using bacterial soft templates. CrystEngComm, 2011, 13, 6747.	2.6	26
126	Enhanced Li- and Na-storage in Sb-Graphene nanocomposite anodes. Materials Research Bulletin, 2016, 76, 338-343.	5.2	26

8

#	Article	IF	CITATIONS
127	Carbon-encapsulated multi-phase nanocomposite of W <sub>2</sub> C@WC <sub>1â^'x</sub> as a highly active and stable electrocatalyst for hydrogen generation. Nanoscale, 2018, 10, 21123-21131.	5.6	26
128	Synthesis and characterization of uniform hollow TiO2 nanofibers using electrospun fibrous cellulosic templates for lithium-ion battery electrodes. Journal of Alloys and Compounds, 2019, 800, 483-489.	5.5	26
129	Electrospun-cellulose derived free-standing carbon nanofibers as lightweight, ultrathin, and stackable interlayers for lithium-sulfur batteries. Chemical Engineering Journal, 2021, 405, 126596.	12.7	26
130	The Reversible Phase Transition and Dielectric Properties of BaNb2O6Polymorphs. Japanese Journal of Applied Physics, 2002, 41, 6045-6048.	1.5	25
131	Mixture behavior and microwave dielectric properties of (1â^'x)Ca2P2O7–xTiO2. Journal of the European Ceramic Society, 2006, 26, 2007-2010.	5.7	25
132	Surface-area-tuned, quantum-dot-sensitized heterostructured nanoarchitectures for highly efficient photoelectrodes. Nano Research, 2014, 7, 144-153.	10.4	25
133	Superior sodium storage performance of reduced graphene oxide-supported Na <sub>3.12</sub> Fe <sub>2.44</sub> (P <sub>2</sub> O <sub>7</sub> ) <sub>2</sub> /C nanocomposites. Chemical Communications, 2017, 53, 9316-9319.	4.1	25
134	Silica-templated hierarchically porous carbon modified separators for lithium–sulfur batteries with superior cycling stabilities. Journal of Power Sources, 2020, 448, 227462.	7.8	25
135	Dynamic evolution of a hydroxylated layer in ruthenium phosphide electrocatalysts for an alkaline hydrogen evolution reaction. Journal of Materials Chemistry A, 2020, 8, 5655-5662.	10.3	25
136	Elucidating the Synergistic Behavior of Orientationâ€Controlled SnS Nanoplates and Carbon Layers for Highâ€Performance Lithium―and Sodiumâ€ion Batteries. Advanced Energy Materials, 2022, 12, .	19.5	25
137	Direct Assembly of BaTiO3-Poly(methyl methacrylate) Nanocomposite Films. Macromolecular Rapid Communications, 2006, 27, 1821-1825.	3.9	24
138	Synthesis and characterization of LiMnBO3 cathode material for lithium ion batteries. Current Applied Physics, 2013, 13, 1440-1443.	2.4	24
139	Comparison of the toxicity of aluminum oxide nanorods with different aspect ratio. Archives of Toxicology, 2015, 89, 1771-1782.	4.2	24
140	Comparison of distribution and toxicity following repeated oral dosing of different vanadium oxide nanoparticles in mice. Environmental Research, 2016, 150, 154-165.	7.5	24
141	Thermally reduced <scp>rGO</scp> â€wrapped CoP/Co <sub>2</sub> P hybrid microflower as an electrocatalyst for hydrogen evolution reaction. Journal of the American Ceramic Society, 2018, 101, 3749-3754.	3.8	24
142	Heteroepitaxy-Induced Rutile VO <sub>2</sub> with Abundantly Exposed (002) Facets for High Lithium Electroactivity. ACS Energy Letters, 2016, 1, 216-224.	17.4	23
143	Comparative study on ternary spinel cathode Zn–Mn–O microspheres for aqueous rechargeable zinc-ion batteries. Journal of Alloys and Compounds, 2019, 800, 478-482.	5.5	23
144	Cellulose-derived tin-oxide-nanoparticle-embedded carbon fibers as binder-free flexible Li-ion battery anodes. Cellulose, 2019, 26, 2557-2571.	4.9	23

#	Article	IF	CITATIONS
145	Superior long-term cycling stability of SnO <sub>2</sub> nanoparticle/multiwalled carbon nanotube heterostructured electrodes for Li-ion rechargeable batteries. Nanotechnology, 2012, 23, 465402.	2.6	22
146	Finite Element Investigation for Edge Wave Prediction in Hot Rolled Steel during Run Out Table Cooling. ISIJ International, 2014, 54, 1646-1652.	1.4	22
147	Comparison of catalytic performance of different types of graphene in Li–O2 batteries. Journal of Alloys and Compounds, 2015, 647, 231-237.	5.5	22
148	Li2MnSiO4 nanorods-embedded carbon nanofibers for lithium-ion battery electrodes. Electrochimica Acta, 2015, 180, 756-762.	5.2	22
149	Enhanced Lithium Storage in Reduced Graphene Oxide-supported M-phase Vanadium(IV) Dioxide Nanoparticles. Scientific Reports, 2016, 6, 30202.	3.3	22
150	Enhanced cycle stability of silicon coated with waste poly(vinyl butyral)-directed carbon for lithium-ion battery anodes. Journal of Alloys and Compounds, 2017, 698, 525-531.	5.5	22
151	Redox effect of Fe2+/Fe3+ in iron phosphates for enhanced electrocatalytic activity in Li-O2 batteries. Chemical Engineering Journal, 2020, 388, 124294.	12.7	22
152	Blood clot-inspired viscoelastic fibrin gel: New aqueous binder for silicon anodes in lithium ion batteries. Energy Storage Materials, 2022, 45, 730-740.	18.0	22
153	Self-supported multi-walled carbon nanotube-embedded silicon nanoparticle films for anodes of Li-ion batteries. Materials Research Bulletin, 2013, 48, 1732-1736.	5.2	21
154	Comparison of toxicity of different nanorodâ€ŧype TiO <sub>2</sub> polymorphs <i>in vivo</i> and <i>in vitro</i> . Journal of Applied Toxicology, 2014, 34, 357-366.	2.8	21
155	Carbon-decorated iron oxide hollow granules formed using a silk fibrous template: lithium-oxygen battery and wastewater treatment applications. NPG Asia Materials, 2017, 9, e450-e450.	7.9	21
156	Nickel disulfide nanosheet as promising cathode electrocatalyst for long-life lithium–oxygen batteries. Energy Storage Materials, 2020, 24, 594-601.	18.0	21
157	Toxicity of orally administered foodâ€grade titanium dioxide nanoparticles. Journal of Applied Toxicology, 2021, 41, 1127-1147.	2.8	21
158	Low-Temperature Sintering of V2O5-Added and -Substituted ZnNb2O6Microwave Ceramics. Japanese Journal of Applied Physics, 2004, 43, 3511-3515.	1.5	20
159	Voltage-Tunable Dielectric Properties of Pyrochlore Bi–Zn–Nb–Ti–O Solid-Solution Thin Films. Japanese Journal of Applied Physics, 2005, 44, 6648-6653.	1.5	20
160	High rate capabilities induced by multi-phasic nanodomains in iron-substituted calcium cobaltite electrodes. Journal of Materials Chemistry, 2009, 19, 1829.	6.7	20
161	Luminescent properties of phosphor converted LED using an orange-emitting Rb2CaP2O7:Eu2+ phosphor. Materials Research Bulletin, 2012, 47, 4522-4526.	5.2	20
162	Facile synthesis of nano-Li4 Ti5O12 for high-rate Li-ion battery anodes. Nanoscale Research Letters, 2012, 7, 10.	5.7	20

#	Article	IF	CITATIONS
163	Nanocomposite Li-ion battery anodes consisting of multiwalled carbon nanotubes that anchor CoO nanoparticles. Materials Letters, 2013, 104, 13-16.	2.6	20
164	Synthesis of Multiphase Cu <sub>3</sub> Ge/GeO <sub><i>x</i></sub> /CuGeO <sub>3</sub> Nanowires for Use as Lithiumâ€lon Battery Anodes. ChemElectroChem, 2014, 1, 673-678.	3.4	20
165	Influence of V2O5 substitutions to Bi2(Zn1/3Nb2/3)2O7 pyrochlore on sintering temperature and dielectric properties. Ceramics International, 2004, 30, 1187-1190.	4.8	19
166	Sintering Behavior and Microwave Dielectric Properties of Tricalcium Phosphate Polymorphs. Japanese Journal of Applied Physics, 2007, 46, 2999-3003.	1.5	19
167	Tailoring nanobranches in three-dimensional hierarchical rutile heterostructures: a case study of TiO2–SnO2. CrystEngComm, 2013, 15, 2939.	2.6	19
168	One-pot synthesis of Fe3O4/Fe/MWCNT nanocomposites via electrical wire pulse for Li ion battery electrodes. Journal of Alloys and Compounds, 2014, 606, 204-207.	5.5	19
169	Ru2P nanofibers for high-performance anion exchange membrane water electrolyzer. Chemical Engineering Journal, 2021, 420, 130491.	12.7	19
170	Metal–organic-framework-derived vanadium( <scp>iii</scp> ) phosphate nanoaggregates for zinc-ion battery cathodes with long-term cycle stability. Journal of Materials Chemistry A, 2022, 10, 10638-10650.	10.3	19
171	Origin of a Shrinkage Anomaly in Anatase. Journal of the American Ceramic Society, 1998, 81, 1692-1694.	3.8	18
172	A numerical model for vacuum carburization of an automotive gear ring. Metals and Materials International, 2011, 17, 885-890.	3.4	18
173	Electrospun Cu/Sn/C Nanocomposite Fiber Anodes with Superior Usable Lifetime for Lithium―and Sodiumâ€Ion Batteries. Chemistry - an Asian Journal, 2014, 9, 3313-3318.	3.3	18
174	Ta-substituted SnNb <sub>2â^'x</sub> Ta <sub>x</sub> O <sub>6</sub> photocatalysts for hydrogen evolution under visible light irradiation. Journal of Materials Chemistry A, 2015, 3, 825-831.	10.3	18
175	A synergistic engineering layer with a versatile H <sub>2</sub> Ti <sub>3</sub> O <sub>7</sub> electrocatalyst for a suppressed shuttle effect and enhanced catalytic conversion in lithium–sulfur batteries. Journal of Materials Chemistry A, 2020, 8, 25411-25424.	10.3	18
176	Separators Modified Using MoO <sub>2</sub> @Carbon Nanotube Nanocomposites as Dual-Mode Li-Polysulfide Anchoring Materials for High-Performance Anti-Self-Discharge Lithium–Sulfur Batteries. ACS Sustainable Chemistry and Engineering, 2020, 8, 15134-15148.	6.7	18
177	Metal organic framework-based nanostructure materials: applications for non-lithium ion battery electrodes. CrystEngComm, 2022, 24, 2925-2947.	2.6	18
178	Template-free synthesis of monodispersed Y3Al5O12:Ce3+ nanosphere phosphor. Journal of Materials Chemistry, 2012, 22, 12275.	6.7	17
179	Hydrothermal Realization of a Hierarchical, Flowerlike MnWO <sub>4</sub> @MWCNTs Nanocomposite with Enhanced Reversible Li Storage as a New Anode Material. Chemistry - an Asian Journal, 2013, 8, 2851-2858.	3.3	17
180	Oleic-acid-assisted carbon coating on Sn nanoparticles for Li ion battery electrodes with long-term cycling stability. RSC Advances, 2014, 4, 44563-44567.	3.6	17

#	Article	IF	CITATIONS
181	Stable high-areal-capacity nanoarchitectured germanium anodes on three-dimensional current collectors for Li ion microbatteries. Journal of Materials Chemistry A, 2016, 4, 1060-1067.	10.3	17
182	Synthesis of Cu <sub>3</sub> (MoO <sub>4</sub> ) <sub>2</sub> (OH) <sub>2</sub> nanostructures by simple aqueous precipitation: understanding the fundamental chemistry and growth mechanism. CrystEngComm, 2017, 19, 154-165.	2.6	17
183	Fabrication of highly porous carbon as sulfur hosts using waste green tea bag powder for lithium–sulfur batteries. Ceramics International, 2017, 43, 2836-2841.	4.8	17
184	Oxygen-vacancy-modified brookite TiO2 nanorods as visible-light-responsive photocatalysts. Materials Letters, 2018, 232, 146-149.	2.6	17
185	Enhancement of Field-Emission Properties in ZnO Nanowire Array by Post-Annealing in H <sub>2</sub> Ambient. Journal of Nanoscience and Nanotechnology, 2009, 9, 4328-4332.	0.9	16
186	Preparation and characterization of nano-sized Y3Al5O12:Ce3+ phosphor by high-energy milling process. Current Applied Physics, 2013, 13, S69-S74.	2.4	16
187	Examination of graphene nanoplatelets as cathode materials for lithium–oxygen batteries by differential electrochemical mass spectrometry. Electrochemistry Communications, 2015, 57, 39-42.	4.7	16
188	Germanium microflower-on-nanostem as a high-performance lithium ion battery electrode. Scientific Reports, 2014, 4, 6883.	3.3	16
189	Carbon-coated tungsten diselenide nanosheets uniformly assembled on porous carbon cloth as flexible binder-free anodes for sodium-ion batteries with improved electrochemical performance. Journal of Alloys and Compounds, 2020, 827, 154348.	5.5	16
190	Orthorhombically distorted perovskite SeZnO3 nanosheets as an electrocatalyst for lithium-oxygen batteries. Chemical Engineering Journal, 2021, 406, 126896.	12.7	16
191	Synthesis and photoactivity of hetero-nanostructured SrTiO3. Journal of the Ceramic Society of Japan, 2010, 118, 876-880.	1.1	15
192	Synthesis of cuprous oxide nanocomposite electrodes by room-temperature chemical partial reduction. Dalton Transactions, 2011, 40, 9498.	3.3	15
193	Synthesis of graphene nanosheets by the electrolytic exfoliation of graphite andÂtheir direct assembly for lithium ion battery anodes. Materials Chemistry and Physics, 2012, 135, 309-316.	4.0	15
194	Fabrication of core/shell ZnWO4/carbon nanorods and their Li electroactivity. Nanoscale Research Letters, 2012, 7, 9.	5.7	15
195	Facile synthesis of heterogeneous Ni-Si@C nanocomposites as high-performance anodes for Li-ion batteries. Electrochimica Acta, 2014, 146, 60-67.	5.2	15
196	One-pot low-temperature sonochemical synthesis of CuO nanostructures and their electrochemical properties. Ceramics International, 2016, 42, 19454-19460.	4.8	15
197	Li-electroactivity of thermally-reduced V2O3 nanoparticles. Materials Letters, 2016, 180, 243-246.	2.6	15
198	Fabrication of sulfur-impregnated porous carbon nanostructured electrodes via dual-mode activation for lithium–sulfur batteries. Materials Letters, 2016, 172, 116-119.	2.6	15

#	Article	IF	CITATIONS
199	Microwave Dielectric Properties of Bi2(Zn1/3Ta2/3)2O7Polymorphs. Japanese Journal of Applied Physics, 2003, 42, 5172-5175.	1.5	14
200	Microwave dielectric properties and Far-infrared spectroscopic analysis of Ba5+nTinNb4O15+3n (0.3 <n<1.2) 2007,="" 27,="" 3081-3086.<="" ceramic="" ceramics.="" european="" journal="" of="" society,="" td="" the=""><td>5.7</td><td>14</td></n<1.2)>	5.7	14
201	Reversible Li-storage in Titanium(III) Oxide Nanosheets. Electrochimica Acta, 2015, 170, 25-32.	5.2	14
202	Synthesis of Silicon Carbide Nanocrystals Using Waste Poly(vinyl butyral) Sheet. Journal of the American Ceramic Society, 2016, 99, 1885-1888.	3.8	14
203	Electrocatalytic performance of CuO/graphene nanocomposites for Li–O 2 batteries. Journal of Alloys and Compounds, 2017, 707, 275-280.	5.5	14
204	Single and polycrystalline CeO <sub>2</sub> nanorods as oxygen-electrode materials for lithium–oxygen batteries. Nanoscale, 2018, 10, 21292-21297.	5.6	14
205	Lowâ€Temperature Synthesis of Phaseâ€Pure 0D–1D BaTiO <sub>3</sub> Nanostructures Using H <sub>2</sub> Ti <sub>3</sub> O <sub>7</sub> Templates. European Journal of Inorganic Chemistry, 2010, 2010, 1343-1347.	2.0	13
206	A novel green-emitting Ca15(PO4)2(SiO4)6:Eu2+ phosphor for applications in n-UV based w-LEDs. Materials Chemistry and Physics, 2013, 139, 350-354.	4.0	13
207	Growth of anatase and rutile TiO2@Sb:SnO2 heterostructures and their application in photoelectrochemical water splitting. International Journal of Hydrogen Energy, 2014, 39, 17508-17516.	7.1	13
208	Sheet-type titania, but not P25, induced paraptosis accompanying apoptosis in murine alveolar macrophage cells. Toxicology Letters, 2014, 230, 69-79.	0.8	13
209	Synthesis of uniform-sized zeolite from windshield waste. Materials Chemistry and Physics, 2015, 166, 20-25.	4.0	13
210	Facile synthesis and electroactivity of 3-D hierarchically superstructured cobalt orthophosphate for lithium-ion batteries. Journal of Alloys and Compounds, 2015, 652, 100-105.	5.5	13
211	A higher aspect ratio enhanced bioaccumulation and altered immune responses due to intravenously-injected aluminum oxide nanoparticles. Journal of Immunotoxicology, 2016, 13, 439-448.	1.7	13
212	Waste Liquid-Crystal Display Glass-Directed Fabrication of Silicon Particles for Lithium-Ion Battery Anodes. ACS Sustainable Chemistry and Engineering, 2019, 7, 15329-15338.	6.7	13
213	Efficient waste polyvinyl(butyral) and cellulose composite enabled carbon nanofibers for oxygen reduction reaction and water remediation. Applied Surface Science, 2020, 510, 145505.	6.1	13
214	Rational design of S, N Co-doped reduced graphene oxides/pyrrhotite Fe7S8 as free-standing anodes for large-scale, ultrahigh-rate and long-lifespan Li- and Na-ion batteries. Applied Surface Science, 2021, 540, 148358.	6.1	13
215	Low temperature sintering and microwave dielectric properties of Ba3Ti5Nb6O28 with B2O3 and CuO additions. Journal of Electroceramics, 2006, 17, 439-443.	2.0	12
216	Electrochemical impedance spectroscopic characterization on nano-sized Ca3Co3FeO9 electrode with enhanced capacity retention. Journal of Applied Electrochemistry, 2010, 40, 109-114.	2.9	12

#	Article	IF	CITATIONS
217	Hydrothermal synthesis and electrochemical properties of FeNbO <sub>4</sub> nanospheres. Journal of the Ceramic Society of Japan, 2012, 120, 82-85.	1.1	12
218	Synthesis and Li electroactivity of Fe2P2O7 microspheres composed of self-assembled nanorods. Ceramics International, 2012, 38, 6927-6930.	4.8	12
219	Adsorption of microbial esterases on Bacillus subtilis-templated cobalt oxide nanoparticles. International Journal of Biological Macromolecules, 2014, 65, 188-192.	7.5	12
220	Biomineralized Multifunctional Magnetite/Carbon Microspheres for Applications in Liâ€lon Batteries and Water Treatment. Chemistry - A European Journal, 2015, 21, 4655-4663.	3.3	12
221	Preparation of cobalt nanoparticles from polymorphic bacterial templates: A novel platform for biocatalysis. International Journal of Biological Macromolecules, 2015, 81, 747-753.	7.5	12
222	Multiple pathways of alveolar macrophage death contribute to pulmonary inflammation induced by silica nanoparticles. Nanotoxicology, 2021, 15, 1087-1101.	3.0	12
223	Comparison of subchronic immunotoxicity of four different types of aluminumâ€based nanoparticles. Journal of Applied Toxicology, 2018, 38, 575-584.	2.8	12
224	γ-Al2O3 nanospheres-directed synthesis of monodispersed BaAl2O4:Eu2+ nanosphere phosphors. CrystEngComm, 2013, 15, 4797.	2.6	11
225	Superior high rate capability of size-controlled LiMnPO4/C nanosheets with preferential orientation. RSC Advances, 2015, 5, 100709-100714.	3.6	11
226	Fe-based hybrid electrocatalysts for nonaqueous lithium-oxygen batteries. Scientific Reports, 2017, 7, 9495.	3.3	11
227	Hierarchical Zn <sub>1.67</sub> Mn <sub>1.33</sub> O <sub>4</sub> /graphene nanoaggregates as new anode material for lithium-ion batteries. International Journal of Energy Research, 2019, 43, 1735-1746.	4.5	11
228	Effect of PM10 on pulmonary immune response and fetus development. Toxicology Letters, 2021, 339, 1-11.	0.8	11
229	Photovoltaic powered solar hydrogen production coupled with waste SO2 valorization enabled by MoP electrocatalysts. Applied Catalysis B: Environmental, 2022, 305, 121045.	20.2	11
230	Significant changes in the ferroelectric properties of BiFeO3 modified SrBi2Ta2O9. Applied Physics Letters, 2003, 83, 1602-1604.	3.3	10
231	Fabrication of tin monosulfide nanosheet arrays using laser ablation. Applied Physics A: Materials Science and Processing, 2011, 103, 505-510.	2.3	10
232	Enhanced Cycle Stability of Magnetite/Carbon Nanoparticles for Li Ion Battery Electrodes. Journal of the American Ceramic Society, 2014, 97, 1413-1420.	3.8	10
233	FeSe hollow spheroids as electrocatalysts for high-rate Li–O2 battery cathodes. Journal of Alloys and Compounds, 2021, 856, 158269.	5.5	10
234	Amorphous silica nanoparticle-induced pulmonary inflammatory response depends on particle size and is sex-specific in rats. Toxicology and Applied Pharmacology, 2020, 390, 114890.	2.8	10

#	Article	IF	CITATIONS
235	Facile Hydrothermal Synthesis of SrNb <sub>2</sub> O <sub>6</sub> Nanotubes with Rhombic Cross Sections. Crystal Growth and Design, 2010, 10, 2447-2450.	3.0	9
236	Luminescent Properties of RbSrPO <sub>4</sub> :Eu <sup>2+</sup> Phosphors for Nearâ€UVâ€Based Whiteâ€Lightâ€Emitting Diodes. European Journal of Inorganic Chemistry, 2013, 2013, 4662-4666.	2.0	9
237	Timeâ€dependent bioaccumulation of distinct rodâ€type TiO <sub>2</sub> nanoparticles: Comparison by crystalline phase. Journal of Applied Toxicology, 2014, 34, 1265-1270.	2.8	9
238	Anion-controlled synthesis of TiO2 nano-aggregates for Li ion battery electrodes. Materials Characterization, 2014, 96, 13-20.	4.4	9
239	Three-Dimensional Numerical Model Considering Phase Transformation in Friction Stir Welding of Steel. Metallurgical and Materials Transactions A: Physical Metallurgy and Materials Science, 2015, 46, 6040-6051.	2.2	9
240	Tissue distribution following 28 day repeated oral administration of aluminumâ€based nanoparticles with different properties and the in vitro toxicity. Journal of Applied Toxicology, 2017, 37, 1408-1419.	2.8	9
241	Synthesis of Flowerâ€iike Cu <sub>3</sub> [MoO <sub>4</sub> ] <sub>2</sub> O from Cu <sub>3</sub> (MoO <sub>4</sub> ) <sub>2</sub> (OH) <sub>2</sub> and Its Application for Lithiumâ€ion Batteries: Structureâ€Electrochemical Property Relationships. ChemElectroChem, 2017, 4, 2608-2617.	3.4	9
242	Tailored Porous ZnCo <sub>2</sub> O <sub>4</sub> Nanofibrous Electrocatalysts for Lithium–Oxygen Batteries. Advanced Materials Interfaces, 2018, 5, 1701234.	3.7	9
243	Revisiting the conversion reaction in ultrafine SnO2 nanoparticles for exceptionally high-capacity Li-ion battery anodes: The synergetic effect of graphene and copper. Journal of Alloys and Compounds, 2018, 769, 1113-1120.	5.5	9
244	Fibrin biopolymer hydrogel-templated 3D interconnected Si@C framework for lithium ion battery anodes. Applied Surface Science, 2021, 551, 149439.	6.1	9
245	Ultrafine CoP nanoparticles encapsulated in N/P dual-doped carbon cubes derived from 7,7,8,8-tetracyanoquinodimethane for lithium-ion batteries. Applied Surface Science, 2021, 555, 149716.	6.1	9
246	Enhanced dielectric constant of polymer-matrix composites using nano-BaTiO3 agglomerates. Journal of the Ceramic Society of Japan, 2010, 118, 62-65.	1.1	8
247	Controlled synthesis and Li-electroactivity of rutile TiO2 nanostructure with walnut-like morphology. Dalton Transactions, 2013, 42, 4278.	3.3	8
248	Enhancement of fluorescence by Ce3+ doping in green-emitting Ca15(PO4)2(SiO4)6:Eu2+ phosphor for UV-based w-LEDs. Ceramics International, 2013, 39, 9791-9795.	4.8	8
249	Controlled phase stability of highly Na-active triclinic structure in nanoscale high-voltage Na 2-2x Co 1+x P 2 O 7 cathode for Na-ion batteries. Journal of Power Sources, 2018, 377, 121-127.	7.8	8
250	Fabrication of Mo/MoO2@carbon cloth as a flexible anode for Li-ion batteries using water-stable nanoink. Carbon, 2018, 139, 1160-1164.	10.3	8
251	S,N co-doped reduced graphene oxide sheets with cobalt hydroxide nanocrystals for highly active and stable bifunctional oxygen catalysts. Inorganic Chemistry Frontiers, 2019, 6, 3501-3509.	6.0	8
252	Organogermanium Nanowire Cathodes for Efficient Lithium–Oxygen Batteries. ACS Nano, 2020, 14, 15894-15903.	14.6	8

#	Article	IF	CITATIONS
253	Enhanced hydrogen evolution activities of the hollow <scp>surfaceâ€oxidized</scp> cobalt phosphide nanofiber electrocatalysts in alkaline media. International Journal of Energy Research, 2022, 46, 13035-13043.	4.5	8
254	Highly active and stable electrocatalytic transition metal phosphides ( <scp> Ni <sub>2</sub> P </scp> ) Tj ETC current density. International Journal of Energy Research, 2020, 44, 11894-11907.	2q0 0 0 rgB7 4.5	[ /Overlock 10 7
255	Freeâ€standing molybdenum disulfides on porous carbon cloth for lithiumâ€ion battery anodes. International Journal of Energy Research, 2021, 45, 11329-11337.	4.5	7
256	Progress and Prospects on the Fabrication of Grapheneâ€Based Nanostructures for Energy Storage, Energy Conversion and Biomedical Applications. Chemistry - an Asian Journal, 2021, 16, 1365-1381.	3.3	7
257	Synthesis and Optical Properties in ZnSxSe1-x Alloy Nanowires. Journal of the Korean Physical Society, 2009, 54, 1650-1654.	0.7	7
258	Degradation Mechanism of Dielectric Loss in Barium Niobate Under a Reducing Atmosphere. Journal of the American Ceramic Society, 2006, 89, 3302-3304.	3.8	6
259	Morphological Evolution of CdS Nanowires to Nanosheets. Journal of Nanoscience and Nanotechnology, 2009, 9, 4487-4491.	0.9	6
260	Morphology-controlled solvothermal synthesis of Li2FeSiO4 nanoparticles for Li-ion battery cathodes. Materials Letters, 2015, 160, 507-510.	2.6	6
261	Inhaled underground subway dusts may stimulate multiple pathways of cell death signals and disrupt immune balance. Environmental Research, 2020, 191, 109839.	7.5	6
262	Formation of lamellar body-like structure may be an initiator of didecyldimethylammonium chloride-induced toxic response. Toxicology and Applied Pharmacology, 2020, 404, 115182.	2.8	6
263	Sodiumâ€nickel pyrophosphate as a novel oxygen evolution electrocatalyst in alkaline medium. Journal of the American Ceramic Society, 2020, 103, 4748-4753.	3.8	6
264	TCNQ-derived N/S dual-doped carbon cube electrocatalysts with built-in CoS2 nanoparticles for high-rate lithium-oxygen batteries. Chemical Engineering Journal, 2021, 418, 129367.	12.7	6
265	Bacteria-Mediated Synthesis of Free-Standing Cobalt Oxide Rods. Journal of Nanoscience and Nanotechnology, 2010, 10, 1129-1134.	0.9	5
266	Glass-frit size dependence of densification behavior and mechanical properties of zinc aluminum calcium borosilicate glass-ceramics. Journal of Alloys and Compounds, 2016, 686, 95-100.	5.5	5
267	Wide pH range electrocatalytic hydrogen evolution using molybdenum phosphide nanoparticles uniformly anchored on porous carbon cloth. Ceramics International, 2021, 47, 9347-9353.	4.8	5
268	Three-dimensional construction of electrode materials using TiC nanoarray substrates for highly efficient electrogeneration of sulfate radicals and molecular hydrogen in a single electrolysis cell. Journal of Materials Chemistry A, 2021, 9, 11705-11717.	10.3	5
269	Rational design of porous Ruâ€doped <scp>CuO</scp> nanoarray on carbon cloth: Toward reversible catalyst layer for efficient <scp> Liâ€O <sub>2</sub> </scp> batteries. International Journal of Energy Research, 2022, 46, 8120-8129.	4.5	5
270	Atmospheric Dependence on Dielectric Loss of 1/6Ba <sub>5</sub> Nb <sub>4</sub> O <sub>15</sub> · 5/6BaNb <sub>2</sub> O <sub>6</sub> Ceramics. Journal of the American Ceramic Society, 2003, 86, 795-799.	3.8	4

#	Article	IF	CITATIONS
271	Fabrication and electrochemical performance of Sn-Based nanocomposite fibers via electrospinning. Electronic Materials Letters, 2013, 9, 775-777.	2.2	4
272	Preparation and Characterizations of Lithium Iron Borate Nano-sized Powders via Aerosol and Thermal Process. Current Nanoscience, 2014, 10, 168-170.	1.2	4
273	Enhanced electrochemical performance of carbon-coated Li2MnSiO4 nanoparticles synthesized by tartaric acid-assisted sol–gel process. Ceramics International, 2014, 40, 9413-9418.	4.8	4
274	Synthesis of carbon-incorporated titanium oxide nanocrystals by pulsed solution plasma: electrical, optical investigation and nanocrystals analysis. RSC Advances, 2015, 5, 9497-9502.	3.6	4
275	Transformation plasticity in boron-bearing low carbon steel. Metals and Materials International, 2015, 21, 799-804.	3.4	4
276	Enhanced sodium storage performance of silk fibroinâ€derived hollow iron sulfide with potential window control. International Journal of Energy Research, 2021, 45, 4755-4764.	4.5	4
277	Repeated intratracheal instillation of zinc oxide nanoparticles induced pulmonary damage and a systemic inflammatory response in cynomolgus monkeys. Nanotoxicology, 2021, 15, 621-635.	3.0	4
278	Vertically Aligned Sulfiphilic Cobalt Disulfide Nanosheets Supported on a Free-Standing Carbon Nanofiber Interlayer for High-Performance Lithium–Sulfur Batteries. ACS Sustainable Chemistry and Engineering, 2021, 9, 8487-8496.	6.7	4
279	Vertically aligned Si@reduced graphene oxide frameworks for <scp>binderâ€free highâ€arealâ€capacity Liâ€ion</scp> battery anodes. International Journal of Energy Research, 2021, 45, 9704-9712.	4.5	4
280	A Finite Element Simulation for Induction Heat Treatment of Automotive Drive Shaft. ISIJ International, 2020, 60, 1333-1341.	1.4	4
281	Oneâ€pot aprotic solventâ€enabled synthesis of superionic <scp>Liâ€argyrodite</scp> solid electrolyte. International Journal of Energy Research, 2022, 46, 17644-17653.	4.5	4
282	Influence of Substrates on the Crystal Structure of Pulsed Laser Deposited Pb(Mg1/3Nb2/3)O3–29% PbTiO3 Thin Films. Journal of Materials Research, 2002, 17, 1030-1034.	2.6	3
283	Influence of strain on the dielectric properties of Bi–Zn–Ti–Nb–O solid solution thin films. Journal of the European Ceramic Society, 2006, 26, 2161-2164.	5.7	3
284	Enhanced electroactivity with Li in Fe3O4/MWCNT nanocomposite electrodes. Journal of Alloys and Compounds, 2014, 615, S397-S400.	5.5	3
285	Windshield-waste-driven synthesis of hydroxy sodalite. Journal of the Ceramic Society of Japan, 2015, 123, 1022-1026.	1.1	3
286	High-power lithium-ion capacitor using orthorhombic Nb2O5 nanotubes enabled by cellulose-based electrospun scaffolds. Cellulose, 2020, 27, 9991-10006.	4.9	3
287	Electrochemical Performance of Calcium Cobaltite Nano-Plates. Journal of Nanoscience and Nanotechnology, 2009, 9, 4056-4060.	0.9	2
288	Synthesis and Li electroactivity of dandelion-like nanorutile. Ceramics International, 2013, 39, 3459-3462.	4.8	2

#	Article	IF	CITATIONS
289	Three-Dimensional Hybrid Tin Oxide/Carbon Nanowire Arrays for High-Performance Li Ion Battery Electrodes. Journal of Nanoscience and Nanotechnology, 2016, 16, 10588-10591.	0.9	2
290	Pulmonary glass particles may persist in the lung suppressing function of immune cells. Environmental Toxicology, 2017, 32, 1688-1700.	4.0	2
291	Lithium–Oxygen Batteries: Tailored Porous ZnCo <sub>2</sub> O <sub>4</sub> Nanofibrous Electrocatalysts for Lithium–Oxygen Batteries (Adv. Mater. Interfaces 4/2018). Advanced Materials Interfaces, 2018, 5, 1870015.	3.7	2
292	Synthesis and Li Electroactivity of MnS/Carbon Nanotube Composites. Journal of the Korean Ceramic Society, 2013, 50, 539-544.	2.3	2
293	Porous Lithiophilic Li–Si Alloyâ€Type Interfacial Framework via Selfâ€Discharge Mechanism for Stable Lithium Metal Anode with Superior Rate (Adv. Energy Mater. 37/2021). Advanced Energy Materials, 2021, 11, 2170146.	19.5	2
294	Lithium Electroactivity of Cobalt Oxide Nanoparticles Synthesized Using Thermolysis Process. Journal of the Korean Ceramic Society, 2011, 48, 636-640.	2.3	2
295	Three-Dimensional Hierarchical Li <sub>4</sub> Ti <sub>5</sub> O <sub>12</sub> Nanoarchitecture by a Simple Hydrothermal Method. Journal of Nanoscience and Nanotechnology, 2014, 14, 9307-9312.	0.9	1
296	Lithium‣ulfur Batteries: "Brainâ€Coralâ€Like―Mesoporous Hollow CoS <sub>2</sub> @Nâ€Doped Graph Carbon Nanoshells as Efficient Sulfur Reservoirs for Lithium–Sulfur Batteries (Adv. Funct. Mater.) Tj ETQq0 0 0	itic rg <b>B4.9</b> 0ve	rlack 10 Tf 50
297	Elucidating the Synergistic Behavior of Orientationâ€Controlled SnS Nanoplates and Carbon Layers for Highâ€Performance Lithium―and Sodiumâ€ŀon Batteries (Adv. Energy Mater. 8/2022). Advanced Energy Materials, 2022, 12, .	19.5	1
298	Porous carbon cubes decorated with cobalt nanoparticles for oxygen evolution catalysis in Znâ€air batteries. International Journal of Energy Research, 2022, 46, 6755-6765.	4.5	1
299	Crystal growth in the low-temperature deposition of polycrystalline silicon thin film. Journal of Crystal Growth, 2005, 274, 347-354.	1.5	Ο
300	A textured barium niobate with enhanced temperature stability of dielectric constant for high-frequency applications. Journal of Materials Research, 2006, 21, 2354-2360.	2.6	0
301	Mechanically Interlocked Polymer Electrolyte with Builtâ€in Fast Molecular Shuttles for Allâ€6olidâ€5tate Lithium Batteries (Adv. Energy Mater. 44/2021). Advanced Energy Materials, 2021, 11, 2170173.	19.5	0
302	Back Cover Image. InformaÄnÃ-Materiály, 2021, 3, .	17.3	0

302 Back Cover Image. InformaAnA-MateriA; Iy, 2021, 3, .